Lund jet plane for Higgs tagging

Charanjit K. Khosa

Dipartimento di Fisica, Università di Genova and INFN, Sezione di Genova, Via Dodecaneso 33, 16146, Italy
charanjit.kaur@ge.infn.it

January 19, 2022

50th International Symposium on Multiparticle Dynamics (ISMD2021)
12-16 July 2021
doi:10.21468/SciPostPhysProc.?

arXiv:2110.15135v2 [hep-ph] 17 Jan 2022

Abstract

We study the boosted Higgs tagging using the Lund jet plane. The convolutional neural network is used for the Lund images data set to classify hadronically decaying Higgs from the QCD background. We consider $H \to b\bar{b}$ and $H \to gg$ decay for moderate and high Higgs transverse momentum and compare the performance with the cut based approach using the jet color ring observable. The approach using Lund plane images provides good tagging efficiency for all the cases.

1 Introduction

Improved Higgs tagging will be beneficial for new physics searches as well as for precise standard model measurements at the Large Hadron Collider (LHC). Recent developments for Higgs tagging explored the potential of Machine Learning (ML) techniques along with novel observable construction, see e.g. [1, 2]. Idea of using ML for jet tagging using low-level raw information (jet images) has been suggested a couple of years ago. We consider Lund jet images and Convolutional Neural Networks (CNN)[1] for the signal and background classification for hadronically decaying boosted Higgs boson [3]. The Lund jet plane is a theory inspired jet representation which is used for jet tagging recently [4, 5][2]. It uses the information of the radiation pattern inside the jet and is a log-log $(\ln\frac{1}{\Delta}, \ln\frac{k_t}{\text{GeV}})$ plane of the angle of the emission and the transverse momentum w.r.t the jet. We consider the primary Lund jet plane. We assess the performance of this approach for both $H \to b\bar{b}$ and $H \to gg$ using two p_T benchmarks (250 GeV and 550 GeV). We compare the classification accuracy with the standard cut based approach where one would consider observables. We consider a single observable named jet color ring, which by construction is an optimal observable for (two-prong) color singlet tagging [10]. It is defined as

$$\mathcal{O} = \frac{\Delta_{ka}^2 + \Delta_{kb}^2}{\Delta_{ab}^2} \tag{1}$$

[1] CNNs provide very efficient image classification for different types of input data in High Energy Physics see e.g. [6,7]
[2] For experimental measurement of the Lund jet plane density see [8, 9].

where a and b are the primary (leading or tagged according to the decay products properties) subject, k is the remaining leading subject and Δ is the separation in the rapidity-azimuth plane.

In our analysis, signal process we consider is $pp \to ZH$ where $Z \to \mu^+\mu^-$ and $H \to b\bar{b}$ or gg, and background processes are Zbb and Zjj for the $H \to b\bar{b}$ and $H \to gg$ analyses, respectively. We simulate events with generation level $p_T^{\mu\mu}$ cut of 200 and 500 GeV using MADGRAPH 2.7.2 [11] at $\sqrt{s} = 14$ TeV. Pseudo-rapidity cuts for leptons ($|\eta_l|$ <2.5) and jets ($|\eta_j|$ <5.0) are also imposed at the generation level. PYTHIA 8.303 [12] (with default Monash 2013 tune [13]) is used for the parton-shower and the hadronization.

We consider the particles excluding muons from Z decay and form radius R=1 jets using the anti-k_t algorithm [14] implementation in FASTJET 3.3.3 [15]. We consider the leading jet with a p_T cut of 250 GeV (or 550 GeV) and jet mass 110 GeV $< m_J <$ 140 GeV for the analysis. We further need to identify the subjects inside the jet for the jet color ring. For that, we cluster the charged particles with p_T >500 MeV using anti-k_t algorithm (radius R=0.2) and form sub-jets. For sub-jets with $p_T > 5$ GeV, we check if the $\Delta < 0.8$ with the leading large radius jet. For the $H \to b\bar{b}$ analysis, we further identify these subjets as b-jets if Δ separation with the large radius jet is less than 0.2. Analysis efficiency is different for the signal and background processes as well as for different p_T benchmarks. A large sample of events is generated such that after selections we get at-least 100K events for all the data sets. We re-cluster the constituents of the large radius jet using C/A algorithm, and consider the declustering history of this jet to get the primary Lund jet plane. We consider 25 by 25 pixels for the Lund jet images. For the CNN training, the data set of 200 K (equal proportions) signal and background events is divided into three sets: training set, validation set and test set in 60:20:20 ratios.

2 H $\to b\bar{b}$ Analysis

Averaged Lund jet plane images and jet color ring distributions of the signal and background are shown in Fig. 1 for both the p_T benchmark points (BPs). The main difference in the Lund plane images is in the high k_T and large Δ region between the two p_T benchmarks. Last column in Fig. 1 has the jet color ring signal and background distributions. Signal jet color ring distributions are peaked towards the lower values and background distributions are comparatively flat. The CNN architecture is presented in Table 1. These benchmarks are labelled as BP1 ($p_T > 250$ GeV) and BP2 ($p_T > 550$ GeV). We compare the Receiver Operating Characteristic (ROC) curves AUC[3] in Fig. 2. We can see CNN classification accuracy for the Lund jet images is slightly better than that of using a cut on the jet color ring (which by construction is an optimal observable to tag a color singlet).

3 H $\to$ gg Analysis

Lund jet plane averaged images and jet color ring distributions are given in Fig. 3. We can easily spot the difference between the signal and background Lund jet images however, jet color ring distributions are almost overlapping. Signal distributions are the same as that of $H \to b\bar{b}$ analysis but the background distributions are very different. In this case several possible color configurations are contributing to the background, contrary to the earlier case where the background was

[3] AUC is the area under the curve. Note that we use $\mathcal{A}$=1-AUC as a performance measure.

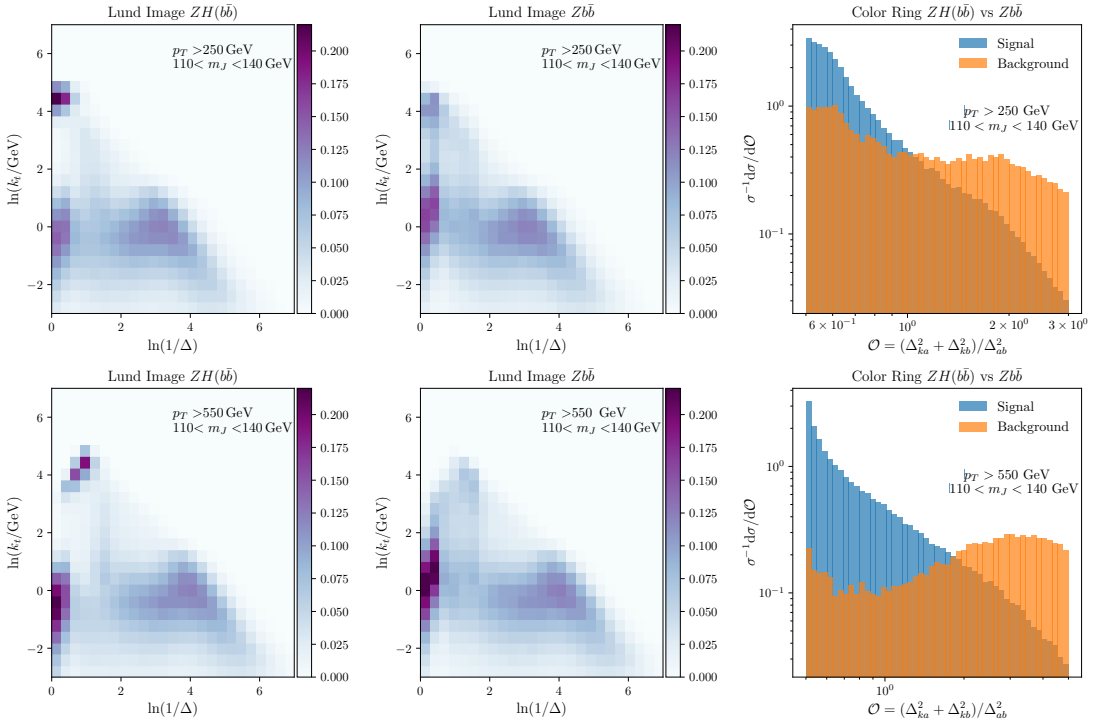


Figure 1: The averaged primary Lund jet plane images and the jet color ring distributions for the $p_T > 250$ GeV and 550 GeV benchmarks of $H \to b\bar{b}$ analysis. Figures are taken from Ref [3] under the Creative Commons Attribution 4.0 International license.

	BP1	BP2	BP3	BP4
N_1 Conv2D	16	16	16	16
N_2 Conv2D	16	16	16	16
Dropouts	0.25	0.05	0.20	0.20
N_3 Conv2D	32	16	16	32
N_4 Conv2D	32	16	16	32
Dropouts	-	0.05	0.30	0.30
Flat Layer	800	800	800	800
Epochs	15	15	20	20
Batch Size	1000	1000	800	700

Table 1: CNN architectures used for different data sets. Here N_i, i =1,..4 represents the number of filters in the i^{th} convolutional layer.

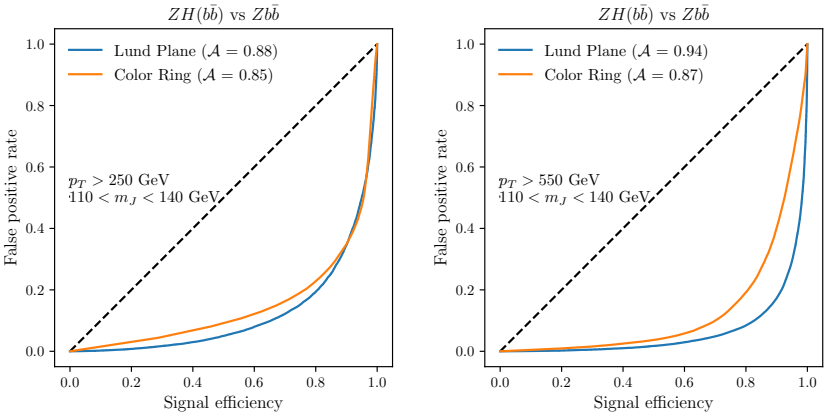


Figure 2: CNN (used for the Lund jet plane images) and color ring ROC curves for $H \to b\bar{b}$ analysis [3].

mainly due to $g \to b\bar{b}$ splitting. As shown in Fig. 4, in this case color ring offers no distinction but CNN can efficiently distinguish the signal and the background. CNN architecture for 250 GeV and 550 GeV benchmark is given by BP3 and BP4 columns in Table 1.

4 Conclusions

We consider the Lund jet plane for Higgs tagging. Using CNN for the signal-background classification, we compare the performance of this set-up with the jet color ring observable. We found the Lund plane and CNN combination provides equally good tagging efficiency for the $H \to b\bar{b}$ and $H \to gg$ analysis. For the first case, the jet color ring also provides similar tagging performance, but it does not offer any separation for the $H \to gg$ decay. This study further motivates the combined analysis of color sensitive observables and Lund jet plane for the optimal Higgs tagging.

Acknowledgements

I thank Simone Marzani for the collaboration on the work presented here. This work is supported by Università di Genova under the curiosity-driven grant "Using jets to challenge the Standard Model of particle physics" and by the Italian Ministry of Research (MUR) under grant PRIN 20172LNEEZ.

References

[1] S. Marzani, G. Soyez and M. Spannowsky, Lect. Notes Phys. **958** (2019), pp, [arXiv:1901.10342 [hep-ph]].

[2] J. Lin, M. Freytsis, I. Moult and B. Nachman, JHEP **10** (2018), 101, [arXiv:1807.10768 [hep-ph]].

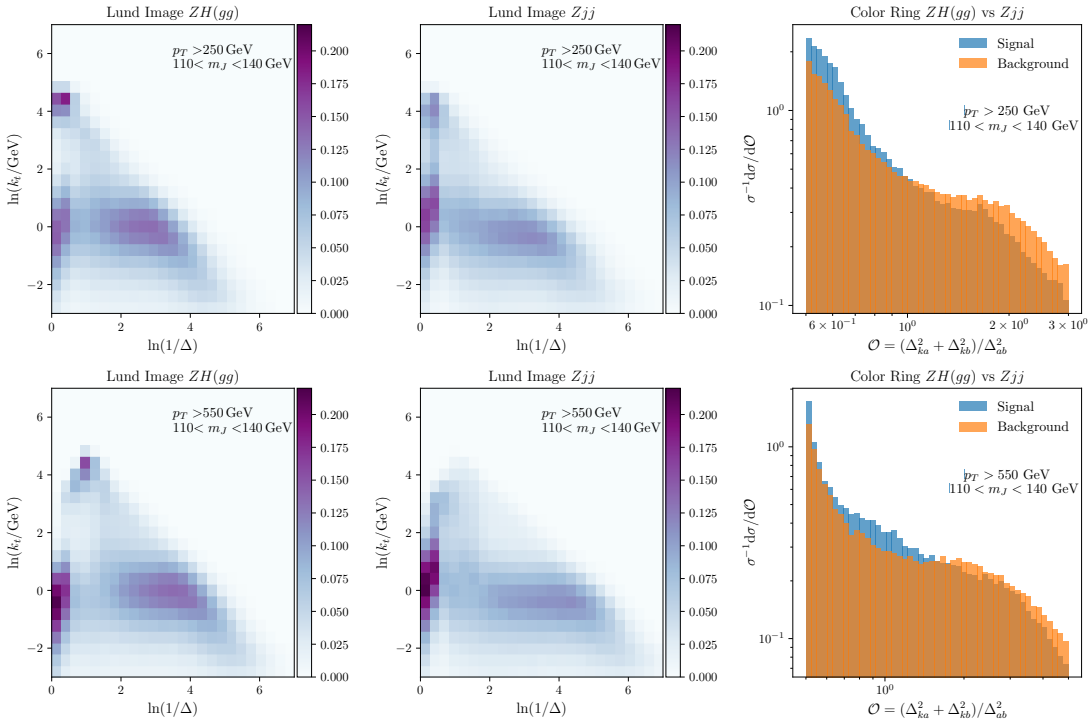


Figure 3: The averaged primary Lund jet plane images and the jet color ring distributions for the $p_T > 250$ GeV and $p_T > 550$ GeV benchmarks of $H \to gg$ analysis. Figures are taken from Ref [3].

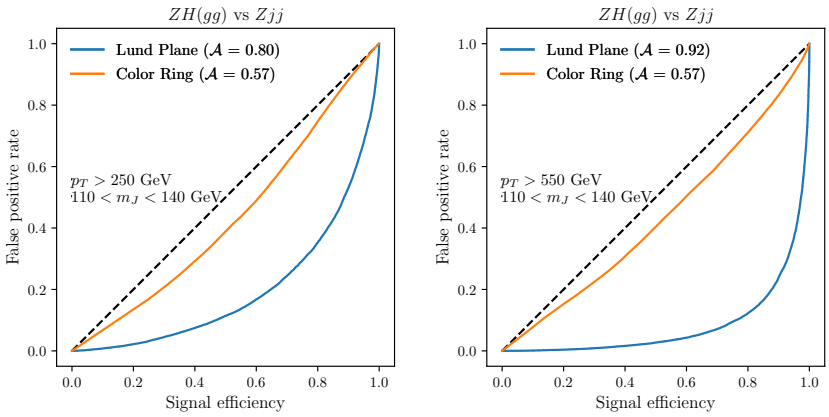


Figure 4: CNN (used for the Lund jet plane images) and color ring ROC curves for the $H \to gg$ analysis [3].

[3] C. K. Khosa and S. Marzani, Phys. Rev. D **104** (2021) no.5, 055043, [arXiv:2105.03989 [hep-ph]].

[4] F. A. Dreyer, G. P. Salam and G. Soyez, JHEP **12** (2018), 064, [arXiv:1807.04758 [hep-ph]].

[5] F. A. Dreyer and H. Qu, JHEP **03** (2021), 052, [arXiv:2012.08526 [hep-ph]].

[6] C. K. Khosa, L. Mars, J. Richards and V. Sanz, J. Phys. G **47** (2020) no.9, 095201, [arXiv:1911.09210 [hep-ph]].

[7] C. K. Khosa, V. Sanz and M. Soughton, SciPost Phys. **10** (2021) no.6, 151, [arXiv:1910.06058 [hep-ph]].

[8] G. Aad *et al.* [ATLAS], Phys. Rev. Lett. **124** (2020) no.22, 222002, [arXiv:2004.03540 [hep-ex]].

[9] ALICE, https://cds.cern.ch/record/2759456.

[10] A. Buckley, G. Callea, A. J. Larkoski and S. Marzani, SciPost Phys. **9** (2020), 026, [arXiv:2006.10480 [hep-ph]].

[11] J. Alwall, R. Frederix, S. Frixione, V. Hirschi, F. Maltoni, O. Mattelaer, H. S. Shao, T. Stelzer, P. Torrielli and M. Zaro, JHEP **07** (2014), 079, [arXiv:1405.0301 [hep-ph]].

[12] T. Sjostrand, S. Mrenna and P. Z. Skands, JHEP **05** (2006), 026, [arXiv:hep-ph/0603175 [hep-ph]]; Comput. Phys. Commun. **178** (2008), 852-867, [arXiv:0710.3820 [hep-ph]].

[13] P. Skands, S. Carrazza and J. Rojo, Eur. Phys. J. C **74** (2014) no.8, 3024, [arXiv:1404.5630 [hep-ph]].

[14] M. Cacciari, G. P. Salam and G. Soyez, JHEP **04** (2008), 063, [arXiv:0802.1189 [hep-ph]].

[15] M. Cacciari, G. P. Salam and G. Soyez, Eur. Phys. J. C **72** (2012), 1896, [arXiv:1111.6097 [hep-ph]].